REPORT NO.
UCB/SEMM-97/01

STRUCTURAL ENGINEERING
MECHANICS AND MATERIALS

COMPUTATIONAL METHODS FOR INVERSE DEFORMATIONS IN QUASI-INCOMPRESSIBLE FINITE ELASTICITY

BY

SANJAY GOVINDJEE
and
PAUL A. MIHALIC

FEBRUARY 1997

DEPARTMENT OF CIVIL AND
ENVIRONMENTAL ENGINEERING
UNIVERSITY OF CALIFORNIA
BERKELEY, CALIFORNIA

Computational Methods for Inverse Deformations in Quasi-incompressible Finite Elasticity

SANJAY GOVINDJEE
PAUL A. MIHALIC

Department of Civil and Environmental Engineering
Structural Engineering, Mechanics and Materials
University of California
Berkeley, CA 94720.

Keywords: Inverse Problem, Incompressible, Shape Design

§ Abstract

This paper presents a formulation for incorporating quasi-incompressibility in inverse design problems for finite elastostatics where deformed configurations and Cauchy tractions are known. In the recent paper of GOVINDJEE & MIHALIC [1996, *Comput. Methods Appl. Mech. Engrg.* **136**, 47-57.] a method for solving this class of inverse problems was presented for compressible materials; here we extend this work to the important case of nearly incompressible materials. A displacement-pressure mixed formulation is combined with a penalty method to enforce the quasi-incompressible constraint without locking. Numerical examples are presented and compared to known solutions; further examples present practical applications of this research to active problems in elastomeric component design.

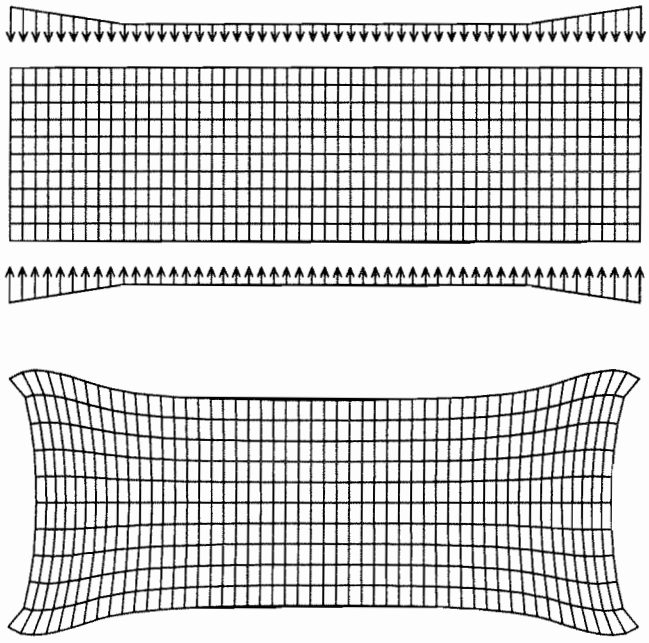

FIGURE 1.1. Top: Deformed gasket cross-section with loading, Bottom: Undeformed gasket cross-section.

§1. Introduction

A problem encountered in the design of finitely deformed elastomeric parts is one in which the initial undeformed shape of a body is unknown and the final deformed shape, applied Cauchy tractions, and displacement boundary conditions are known. The problem being to compute the undeformed shape. For an illustration, consider the design of the "manufactured shape" of a gasket. To prevent leakage, the gasket is required to have an increased clamping force along the edges, and fit into a rectangular region; a cross section of the known deformed gasket is shown in the top of Fig. **1.1**. Computational aspects aside, the gasket to be manufactured must have a cross-sectional shape as shown in the bottom of Fig. **1.1** (where the top and bottom surfaces have been constrained from lateral motion).

This class of problems was studied by SHIELD [1967] who posed the "inverse deformation" problem as a set of balance equations written in terms of the inverse deformation and standard boundary conditions. Later, CHADWICK [1975] showed the existence of various duality relations between the inverse and forward problem. In particular, Chadwick noted

a duality between the Cauchy stress tensor and Eshelby's Energy Momentum tensor; see ESHELBY [1956, 1975]. Using this result, Chadwick recognized that under certain restrictions Shield's equilibrium equations could be formulated in terms of Eshelby's tensor. In contrast to other inverse problems, the inverse deformation problem at hand can be shown to be "well-posed" in accordance with Hadamard's definition.

Recently two numerical methods have been proposed for this class of problems; see GOVINDJEE & MIHALIC [1996] and YAMADA [1995]. In the first paper, the authors present two formulations – one based on Eshelby's Energy Momentum tensor and a second based on a re-parameterization of the equilibrium equations. The energy momentum formulation was shown to be deficient in several regards. In particular, the Energy Momentum formulation places strong continuity requirements on the motion and Eshelby's tensor lacks direct physical connection to the stated problem creating difficulties with the boundary conditions. The re-parameterization approach was shown to require only C^0 continuity and it had a direct physical connection to the problem at hand, eliminating boundary condition difficulties. The resulting numerical formulation was easily implemented using standard (forward) numerical methods. This work has also been shown to be consistent with the less straight–forward formulation of YAMADA [1995]. The main shortcoming of the GOVINDJEE & MIHALIC [1996] paper was its restriction to compressible elasticity. Note that elastomers, the canonical example for finite elasticity, are nearly volume preserving; see for example TRELOAR [1975].

In this paper we propose to remedy this situation by considering a re-parameterization of the weak form of the forward problem of finite elasticity as a solution method for the inverse incompressible problem. Many numerical approaches have been proposed for solving forward problems in incompressible finite elasticity. Most commonly a mixed formulation is assumed with independent fields for displacements, pressure, and sometimes the volumetric deformation. The isochoric constraint is either enforced as near incompressibility or full incompressibility. The former is achieved through penalty methods and the latter through Lagrange multiplier methods; see for example LUENBERGER [1984]. In this work, a displacement-pressure mixed formulation is used in combination with a penalty method to approximately enforce the constraint. The approach is modeled most closely after the

two field formulation of SUSSMAN & BATHE [1987].

The paper is divided into four sections. Section 2 reviews the compressible problem development; Section 3 derives a weak form expression for the incompressible inverse deformation problem; Section 4 develops the finite element formulation for the inverse problem; in Section 5 a set of examples illustrate applications of the method. The approach is also extended to the three field formulation in Appendix A.

§2. Review of the Compressible Problem

2.1. Forward Problem. Let the open set $\mathcal{B} \subset \mathbb{R}^3$ be the reference placement of a continuum body containing the material points $\boldsymbol{X} \in \mathcal{B}$. Points in the reference placement are mapped to the deformed configuration $\mathcal{S} \subset \mathbb{R}^3$ by the motion $\boldsymbol{x} = \boldsymbol{\phi}(\boldsymbol{X})$ where $\mathcal{S} = \boldsymbol{\phi}(\mathcal{B})$ and points in the deformed configuration are denoted by $\boldsymbol{x} \in \mathcal{S}$.

Consider a hyper-elastic material with a strain energy function, $W : \text{Lin}_+ \longrightarrow \mathbb{R}$ per unit reference volume where Lin_+ is the space of second order tensors with positive determinant. We define the deformation gradient as $\boldsymbol{F} = \text{GRAD}(\boldsymbol{\phi})$ where $\text{GRAD}(\cdot)$ denotes the gradient operator with respect to $\boldsymbol{X}$. This leads to an expression for the Cauchy stress tensor as

$$\boldsymbol{\sigma} = \frac{1}{J}\frac{\partial W(\boldsymbol{F})}{\partial \boldsymbol{F}}\boldsymbol{F}^T = \frac{1}{J}\boldsymbol{P}(\boldsymbol{F})\boldsymbol{F}^T \tag{2.1}$$

where $\boldsymbol{P} = \partial W(\boldsymbol{F})/\partial \boldsymbol{F}$ is the first Piola-Kirchhoff stress tensor and $J = \det[\boldsymbol{F}]$. The boundary value problem for the unknown motion $\boldsymbol{\phi}$ is defined by the following equilibrium equations and boundary conditions: for all $\boldsymbol{x} \in \mathcal{S}$

$$\text{div}[\boldsymbol{\sigma}] + \widehat{\boldsymbol{b}} = \boldsymbol{o} \qquad \text{and} \qquad \boldsymbol{\sigma} = \boldsymbol{\sigma}^T; \tag{2.2}$$

for all $\boldsymbol{x} \in \partial\mathcal{S}_t$

$$\boldsymbol{\sigma}\boldsymbol{n} = \bar{\boldsymbol{t}}; \tag{2.3}$$

and for all $\boldsymbol{x} \in \partial\mathcal{S}_\phi$

$$\boldsymbol{\phi} = \bar{\boldsymbol{\phi}}, \tag{2.4}$$

where div[·] is the divergence operator with respect to $\boldsymbol{x}$, $\widehat{\boldsymbol{b}}$ a given body force per unit spatial volume, $\bar{\boldsymbol{t}}$ a given traction function per unit deformed area, $\boldsymbol{n}$ the boundary outward normal, $\bar{\boldsymbol{\phi}}$ a given surface motion, $\partial\mathcal{S}_t \cap \partial\mathcal{S}_\phi = \emptyset$, and $\overline{\partial\mathcal{S}_t \cup \partial\mathcal{S}_\phi} = \partial\mathcal{S}$ the boundary of $\mathcal{S}$.

2.2. Inverse Problem. Let $\boldsymbol{\varphi} = \boldsymbol{\phi}^{-1}$ be the inverse motion. In the inverse problem the primary unknown is the inverse motion $\boldsymbol{\varphi}(\boldsymbol{x})$. We begin by defining a set of duality relations: a strain energy function $w : \mathrm{Lin}_+ \longrightarrow \mathbb{R}$ as $w = W/J$ and an inverse deformation gradient $\boldsymbol{f} = \mathrm{grad}(\boldsymbol{\varphi})$ where grad(·) is the gradient operator with respect to $\boldsymbol{x}$. The inverse deformation gradient is related to its forward dual through the relation $\boldsymbol{f} = \boldsymbol{F}^{-1} \circ \boldsymbol{\varphi}$, where $\circ$ is the composition symbol. The inverse Jacobian is similarly defined as $j = det(\boldsymbol{f}) = 1/J \circ \boldsymbol{\varphi}$. The boundary value problem for the unknown motion $\boldsymbol{\varphi}$ is found through the trivial observation that (2.1) through (2.3) can be re-parameterized in terms of the inverse motion. Also note the displacement boundary condition (2.4) can be prescribed with reference to the inverse motion. Thus, the equilibrium equations and boundary conditions for the inverse problem become: for all $\boldsymbol{x} \in \mathcal{S}$

$$\mathrm{div}[\boldsymbol{\sigma}] + \widehat{\boldsymbol{b}} = \boldsymbol{o} \qquad \text{and} \qquad \boldsymbol{\sigma} = \boldsymbol{\sigma}^T\,, \tag{2.5}$$

for all $\boldsymbol{x} \in \partial\mathcal{S}_t$

$$\boldsymbol{\sigma n} = \bar{\boldsymbol{t}}\,; \tag{2.6}$$

and for all $\boldsymbol{x} \in \partial\mathcal{S}_\varphi$

$$\boldsymbol{\varphi} = \bar{\boldsymbol{\varphi}}\,. \tag{2.7}$$

The constitutive relation may be expressed in terms of the inverse motion as

$$\boldsymbol{\sigma} = j\boldsymbol{P}(\boldsymbol{f}^{-1})\boldsymbol{f}^{-T}\,. \tag{2.8}$$

Remark 2.1.

This approach differs from the approaches of SHIELD [1967] and later CHADWICK [1975] who further defined an inverse dual to (2.1) as

$$\boldsymbol{\Sigma} = \frac{1}{j}\frac{\partial w(\boldsymbol{f})}{\partial \boldsymbol{f}}\boldsymbol{f}^T = \frac{1}{j}\boldsymbol{p}\boldsymbol{f}^T\,, \tag{2.9}$$

where $\boldsymbol{p} = \partial w(\boldsymbol{f})/\partial \boldsymbol{f}$ is the dual to $\boldsymbol{P}$, and $\boldsymbol{\Sigma}$ the dual to $\boldsymbol{\sigma}$. Note, $\boldsymbol{\Sigma}$ can be expanded as $\boldsymbol{\Sigma} = W\mathbf{1} - \boldsymbol{F}^T\boldsymbol{P}$, which is Eshelby's energy-momentum tensor in essentially CHADWICK'S notation and $\mathbf{1}$ is the second order identity tensor; ESHELBY [1975, §5] denotes $\boldsymbol{\Sigma}$ as $\boldsymbol{P}^*$ and CHADWICK [1975] † denotes it $\boldsymbol{\Sigma}^T$. Under the strict assumption of a smooth motion ($\boldsymbol{\phi} \in C^2(\mathcal{B})$), positive Jacobian ($J > 0$), and zero body forces ($\widehat{\boldsymbol{b}} = 0$) this method leads to the conclusion that static equilibrium is satisfied if and only if for all $\boldsymbol{x} \in \mathcal{S}$

$$\operatorname{div}[\boldsymbol{p}] = \boldsymbol{o} \quad \text{and} \quad \boldsymbol{f}\boldsymbol{p}^T = \boldsymbol{p}\boldsymbol{f}^T. \tag{2.10}$$

To complete the statement of the inverse problem, boundary conditions need to be given. For a direct analogy with the forward problem, one could write: for all $\boldsymbol{x} \in \partial\mathcal{S}_t$

$$\boldsymbol{p}\boldsymbol{n} = \bar{\boldsymbol{t}}_{em}\,, \tag{2.11}$$

and for all $\boldsymbol{x} \in \partial\mathcal{S}_\varphi$

$$\boldsymbol{\varphi} = \bar{\boldsymbol{\varphi}}\,, \tag{2.12}$$

where $\bar{\boldsymbol{t}}_{em}$ is a quantity which we will call the energy momentum traction. Note that in comparison to the forward problem $\bar{\boldsymbol{t}}_{em}$ is not directly related to the physically relevant boundary condition. Thus, while equations (2.9) - (2.12) form a complete boundary value problem which can be solved for the inverse motion $\boldsymbol{\varphi}$, the corresponding weak form for these equations involves non-standard terms leading to numerical difficulties; for details see GOVINDJEE & MIHALIC [1996]. Note, also, that the inclusion of body forces in the energy-momentum complicates the formulation substantially. □

§3. Incompressible Problem Description

Consider the standard forward problem of finite elasticity defined by (2.1) - (2.4) and

† The presence of the transpose in Chadwick's notation merely reflects a difference in the convention of which leg of the stress tensor corresponds to the section normal and which leg corresponds to the traction direction.

the added constraint

$$J - 1 = 0. \tag{3.1}$$

The addition of the constraint insures that only isochoric motions occur. Equation (3.1) is referred to as an internal constraint on the material behavior (see for example OGDEN [1984, p. 198]). Numerical approaches for adding a constraint to a boundary value problem include: penalty methods, Lagrange multipliers, or a combinations of both methods. In the formulation presented, a penalty parameter κ will be used in combination with a two-field variational principle.

The numerical phenomena of "locking" associated with problems in incompressible elasticity has been effectively treated using mixed methods. Locking is a purely numerical issue which occurs in finite element methods as a result of over constraining the problem. The two field variational principle provides a basis for the development of a mixed method that prevents locking by approximating the pressure (Lagrange multiplier p) and displacements using independent fields as proposed by SUSSMAN & BATHE [1987]. Other authors have also included the volumetric deformation as a third independent field (SIMO & TAYLOR [1991]). In this work a two-field pressure-displacement formulation will be used. For completeness the pertinent equations for the three field formulation are included in Appendix A. For the examples shown the two field formulation performed satisfactorily.

3.1. Standard Forward Quasi-incompressible Problem. A convenient assumption in quasi-incompressible elasticity is that the deviatoric stresses are caused by purely deviatoric strains. This is achieved in finite deformation elasticity through the use of a multiplicative split of the deformation gradient (FLORY [1961]) into purely volumetric and purely deviatoric parts. The deviatoric and volumetric parts of the deformation gradient are, respectively, defined as

$$\tilde{\boldsymbol{F}} = J^{-1/3}\boldsymbol{F} \tag{3.2}$$

and

$$\boldsymbol{F}_{vol} = J^{1/3}\mathbf{1}. \tag{3.3}$$

Note that $\boldsymbol{F} = \tilde{\boldsymbol{F}}\boldsymbol{F}_{vol}$, $\det(\tilde{\boldsymbol{F}}) = 1$, and $\det(\boldsymbol{F}_{vol}) = J$. These definitions allow us to state

the strong form equations of the forward quasi-incompressible problem as: for all $\boldsymbol{x} \in \mathcal{S}$

$$p = \kappa(J-1), \tag{3.4}$$

and

$$\text{div}[\tilde{\boldsymbol{\sigma}} + p\mathbf{1}] + \widehat{\boldsymbol{b}} = 0 \quad \text{and} \quad \boldsymbol{\sigma} = \boldsymbol{\sigma}^T; \tag{3.5}$$

for all $\boldsymbol{x} \in \partial\mathcal{S}_t$

$$\boldsymbol{\sigma}\boldsymbol{n} = \bar{\boldsymbol{t}}\,, \tag{3.6}$$

and for all $\boldsymbol{x} \in \partial\mathcal{S}_\phi$

$$\phi = \bar{\phi}\,, \tag{3.7}$$

where $\boldsymbol{\sigma} = \tilde{\boldsymbol{\sigma}} + p\mathbf{1}$ is the total stress, $p \in \mathbb{R}$ denotes the pressure, and $\kappa \in \mathbb{R}^+$ is a penalty parameter chosen large. The constitutive relation for the deviatoric portion of the stress is defined over the purely deviatoric motions as:

$$\tilde{\boldsymbol{\sigma}} = \frac{\partial W(\tilde{\boldsymbol{F}})}{\partial \tilde{\boldsymbol{F}}} \tilde{\boldsymbol{F}}^T. \tag{3.8}$$

Remark 3.1.

Note that (3.4) is the multiplication of a penalty parameter (usually chosen large) with the constraint which is approaching zero. The result is a finite value for the pressure p (Lagrange multiplier). □

3.2. Inverse Quasi-incompressible Problem. It is again a trivial observation that we can re-parameterize the (forward) strong form equations (3.4) - (3.8) as a function of the inverse motion $\boldsymbol{\varphi} = \boldsymbol{\phi}^{-1}$. This gives the strong form equations for the inverse incompressible problem as: for all $\boldsymbol{x} \in \mathcal{S}$

$$p = \kappa(1/j - 1), \tag{3.9}$$

and

$$\text{div}[\tilde{\boldsymbol{\sigma}} + p\mathbf{1}] + \widehat{\boldsymbol{b}} = 0 \quad \text{and} \quad \boldsymbol{\sigma} = \boldsymbol{\sigma}^T; \tag{3.10}$$

for all $\boldsymbol{x} \in \partial\mathcal{S}_t$

$$\boldsymbol{\sigma}\boldsymbol{n} = \bar{\boldsymbol{t}}\,; \tag{3.11}$$

for all $\boldsymbol{x} \in \partial\mathcal{S}_\varphi$

$$\boldsymbol{\varphi} = \bar{\boldsymbol{\varphi}}. \tag{3.12}$$

The constitutive relation is given by:

$$\tilde{\boldsymbol{\sigma}} = \boldsymbol{P}(\tilde{\boldsymbol{f}}^{-1})\tilde{\boldsymbol{f}}^{-T}, \tag{3.13}$$

where $\tilde{\boldsymbol{f}} = \tilde{\boldsymbol{F}}^{-1} = j^{-1/3}\boldsymbol{f}$.

The weak form equations for the inverse incompressible problem are obtained by multiplying (3.9)–(3.10) by arbitrary admissible weighting functions, integrating over the domain, and performing integration by parts on the result. The resulting weak form expressions are:

$$\tilde{G}_1(\boldsymbol{\varphi}, p; \boldsymbol{\eta}) = \int_{\mathcal{S}} [\tilde{\boldsymbol{\sigma}} : grad(\boldsymbol{\eta}) + p \ \mathrm{div}(\boldsymbol{\eta})] + G_{ext} = 0 \tag{3.14}$$

and

$$\tilde{G}_2(\boldsymbol{\varphi}, p; \beta) = \int_{\mathcal{S}} [\kappa(\frac{1}{j} - 1) - p]\beta = 0\,. \tag{3.15}$$

where $\boldsymbol{\eta} : \mathcal{S} \longrightarrow \mathbb{R}^3$ and $\boldsymbol{\eta} = 0$ on $\partial\mathcal{S}_\varphi$, $\beta : \mathcal{S} \longrightarrow \mathbb{R}$, and G_{ext} contains the contribution of the tractions $\bar{\boldsymbol{t}}$ and body forces $\widehat{\boldsymbol{b}}$. Note that the pressure-volume expression is given its own variational equation rather than substituting (3.9) into (3.14) and eliminating (3.15). This opens up the possibility to create a mixed finite element formulation.

§4. Finite Element Formulation

The finite element formulation of the weak form problem defined by (3.14) and (3.15) can be solved using suitable approximations to $\boldsymbol{\varphi}$, $\boldsymbol{\eta}$, p, and β. By assuming a constant approximation per element for β and p, we can solve (3.15) explicitly over an individual element e for the pressure p_e as,

$$p_e = \frac{1}{v_e}\int_{\mathcal{S}_e} \kappa(\frac{1}{j} - 1), \tag{4.1}$$

where $\mathcal{S}_e$ refers to an individual element domain and v_e is the "spatial element volume." We can then substitute this result back into (3.14) to arrive at a single weak form expression,

$$G(\boldsymbol{\varphi}; \boldsymbol{\eta}) = \tilde{G}_1(\boldsymbol{\varphi}, p_e(\boldsymbol{\varphi}); \boldsymbol{\eta}) = 0. \tag{4.2}$$

Equation (4.2) represents a system of non-linear equations which can be solved for the motion $\boldsymbol{\varphi}$, given suitable element subspaces for $\boldsymbol{\eta}$ and $\boldsymbol{\varphi}$.

4.1. Linearization. In typical implicit codes a Newton-Raphson method is used to solve (4.2) for the unknown motion. This techniques is based upon the linearization of (4.2) about a current iterate $\boldsymbol{\varphi}^{(k)}$ in the arbitrary direction $\boldsymbol{\nu} : \mathcal{S} \longrightarrow \mathbb{R}^3$, where $\boldsymbol{\nu} = 0$ on $\partial\mathcal{S}_\varphi$. This gives

$$\mathcal{L}G(\boldsymbol{\varphi}^{(k)};\boldsymbol{\eta})[\boldsymbol{\nu}] = G(\boldsymbol{\varphi}^{(k)};\boldsymbol{\eta}) + D_1G(\boldsymbol{\varphi}^{(k)};\boldsymbol{\eta})[\boldsymbol{\nu}]. \tag{4.3}$$

The "element tangent" is given by:

$$\begin{aligned} D_1G(\boldsymbol{\varphi}^{(k)};\boldsymbol{\eta})[\boldsymbol{\nu}] = &\int_{\mathcal{S}_e} 2\,\mathrm{sym}[\mathrm{grad}(\boldsymbol{\eta})] : \mathrm{DEV}\left[\frac{\partial\tilde{\boldsymbol{\sigma}}}{\partial\tilde{\boldsymbol{c}}}\right] : \mathrm{sym}[\boldsymbol{f}^T\mathrm{grad}(\boldsymbol{\nu})] \\ &- \left(\int_{\mathcal{S}_e}\mathrm{div}(\boldsymbol{\eta})\right)\frac{\kappa}{v_e}\left(\int_{\mathcal{B}_e} J^2\mathrm{DIV}(\boldsymbol{\nu})\right), \end{aligned} \tag{4.4}$$

where

$$\mathrm{DEV}[\cdot] = j^{-2/3}\left([\cdot] - \frac{1}{3}\,([\cdot] : \boldsymbol{c})\boldsymbol{c}^{-1}\right), \tag{4.5}$$

$\boldsymbol{c} = \boldsymbol{f}^T\boldsymbol{f}$, $\tilde{\boldsymbol{c}} = \tilde{\boldsymbol{f}}^T\tilde{\boldsymbol{f}}$, and $\mathrm{sym}[\cdot] = 1/2([\cdot] + [\cdot]^T)$. Equation (4.3) may be set to zero and solved for $\boldsymbol{\nu}$ and the iterate updated via the Newton-Raphson formula:

$$\boldsymbol{\varphi}^{(k+1)} = \boldsymbol{\varphi}^{(k)} + \boldsymbol{\nu}\,. \tag{4.6}$$

Remark 4.1.

We note that the first term of (4.4) essentially matches the tangent for the compressible formulation (Govindjee & Mihalic [1996]) and the second term gives the mixed pressure contribution. The lack of symmetry of the second term is consistent with the first term and characteristic of this problem class. □

Remark 4.2.

The resulting procedure provides a general approach for developing the inverse problem for other methods of enforcing incompressibility. For example, we may have instead considered the three field formulation of Simo & Taylor [1991] (see Appendix A). While some of the details change, the general procedure is the same. □

Remark 4.3.

In the case of exact incompressibility, we could have instead chosen to use $1/J - 1 = 0$ as the constraint in contrast to (3.1). This will yield simpler linearizations as seen by (4.1) which would become

$$p_e = \frac{1}{v_e} \int_{\mathcal{S}_e} \kappa(j-1). \tag{4.7}$$

Note the resulting tangent would no longer contain the J^2 in the last integral of (4.4). However, in the quasi-incompressible case the slope of the pressure-volume relation would then be negative. For large values of κ this is immaterial, but for more moderate values this is a crucial point. □

4.2. 3D Matrix Formulation. The terms in the tangent (4.4) can be easily converted to a matrix formulation. Consider the following approximations for the arbitrary variations and solution field:

$$\boldsymbol{\eta} = \sum_{A=1}^{nen} N_A \boldsymbol{\eta}_A, \quad \boldsymbol{\nu} = \sum_{A=1}^{nen} N_A \boldsymbol{\nu}_A, \qquad \text{and} \qquad \boldsymbol{\varphi} = \sum_{A=1}^{nen} N_A \boldsymbol{\varphi}_A, \tag{4.8}$$

where N_A are the shape functions and $\boldsymbol{\eta}_A \in \mathbb{R}^3$, $\boldsymbol{\nu}_A \in \mathbb{R}^3$, and $\boldsymbol{\varphi}_A \in \mathbb{R}^3$ are discrete nodal values with *nen* being the number of element nodes. The discrete nodal values can be arranged in a compact vector form as,

$$\underline{\boldsymbol{\nu}} = [\nu_1^1, \nu_2^1, \nu_3^1, \ldots, \nu_1^{nen}, \nu_2^{nen}, \nu_3^{nen}]^T. \tag{4.9}$$

Define the following block matrices:

$$\begin{aligned}
\underline{\boldsymbol{B}} &= [\boldsymbol{B}_1, \boldsymbol{B}_2, \cdots, \boldsymbol{B}_{nen}], \\
\underline{\boldsymbol{b}} &= [\boldsymbol{b}_1, \boldsymbol{b}_2, \cdots, \boldsymbol{b}_{nen}], \\
\underline{\boldsymbol{f}} &= \mathrm{diag}[\boldsymbol{f}, \boldsymbol{f}, \cdots, \boldsymbol{f}]_{3nen \times 3nen}, \\
\underline{\boldsymbol{F}} &= \mathrm{diag}[\boldsymbol{F}, \boldsymbol{F}, \cdots, \boldsymbol{F}]_{3nen \times 3nen}, \\
\underline{\boldsymbol{c}} &= [c_{11}, c_{22}, c_{33}, 2c_{12}, 2c_{23}, 2c_{13}]^T, \quad \text{and} \\
\underline{\boldsymbol{c}}^{-1} &= [c_{11}^{-1}, c_{22}^{-1}, c_{33}^{-1}, c_{12}^{-1}, c_{23}^{-1}, c_{13}^{-1}]^T,
\end{aligned} \tag{4.10}$$

where

$$\boldsymbol{B}_A = \begin{bmatrix} N_{A,1} & 0 & 0 \\ 0 & N_{A,2} & 0 \\ 0 & 0 & N_{A,3} \\ N_{A,2} & N_{A,1} & 0 \\ 0 & N_{A,3} & N_{A,2} \\ N_{A,3} & 0 & N_{A,1} \end{bmatrix} \qquad \text{and} \qquad \boldsymbol{b}_A = [\, N_{A,1}, N_{A,2}, N_{A,3} \,]\,. \tag{4.11}$$

Using this notation we arrive at the following relations:

$$\begin{aligned} \text{sym}[\text{grad}(\boldsymbol{\eta})] &= \underline{\boldsymbol{B}}\ \underline{\boldsymbol{\eta}}, \\ \text{sym}[\boldsymbol{f}^T \text{grad}(\boldsymbol{\nu})] &= \underline{\boldsymbol{B}}\ \underline{\boldsymbol{f}}^T\ \underline{\boldsymbol{\nu}}, \\ \text{div}[\boldsymbol{\eta}] &= \underline{\boldsymbol{b}}\ \underline{\boldsymbol{\eta}}, \quad \text{and} \\ \text{DIV}[\boldsymbol{\nu}] &= \underline{\boldsymbol{b}}\ \underline{\boldsymbol{F}}\ \underline{\boldsymbol{\nu}}. \end{aligned} \tag{4.12}$$

The material stiffness is mapped to a 6×6 matrix $\underline{\tilde{\boldsymbol{D}}}$ as:

$$\underline{\tilde{\boldsymbol{D}}} = \begin{bmatrix} \partial\tilde{\sigma}_{11}/\partial\tilde{c}_{11} & \partial\tilde{\sigma}_{11}/\partial\tilde{c}_{22} & \partial\tilde{\sigma}_{11}/\partial\tilde{c}_{33} & \partial\tilde{\sigma}_{11}/\partial\tilde{c}_{12} & \partial\tilde{\sigma}_{11}/\partial\tilde{c}_{23} & \partial\tilde{\sigma}_{11}/\partial\tilde{c}_{13} \\ \partial\tilde{\sigma}_{22}/\partial\tilde{c}_{11} & \partial\tilde{\sigma}_{22}/\partial\tilde{c}_{22} & \partial\tilde{\sigma}_{22}/\partial\tilde{c}_{33} & \partial\tilde{\sigma}_{22}/\partial\tilde{c}_{12} & \partial\tilde{\sigma}_{22}/\partial\tilde{c}_{23} & \partial\tilde{\sigma}_{22}/\partial\tilde{c}_{13} \\ \partial\tilde{\sigma}_{33}/\partial\tilde{c}_{11} & \partial\tilde{\sigma}_{33}/\partial\tilde{c}_{22} & \partial\tilde{\sigma}_{33}/\partial\tilde{c}_{33} & \partial\tilde{\sigma}_{33}/\partial\tilde{c}_{12} & \partial\tilde{\sigma}_{33}/\partial\tilde{c}_{23} & \partial\tilde{\sigma}_{33}/\partial\tilde{c}_{13} \\ \partial\tilde{\sigma}_{12}/\partial\tilde{c}_{11} & \partial\tilde{\sigma}_{12}/\partial\tilde{c}_{22} & \partial\tilde{\sigma}_{12}/\partial\tilde{c}_{33} & \partial\tilde{\sigma}_{12}/\partial\tilde{c}_{12} & \partial\tilde{\sigma}_{12}/\partial\tilde{c}_{23} & \partial\tilde{\sigma}_{12}/\partial\tilde{c}_{13} \\ \partial\tilde{\sigma}_{23}/\partial\tilde{c}_{11} & \partial\tilde{\sigma}_{23}/\partial\tilde{c}_{22} & \partial\tilde{\sigma}_{23}/\partial\tilde{c}_{33} & \partial\tilde{\sigma}_{23}/\partial\tilde{c}_{12} & \partial\tilde{\sigma}_{23}/\partial\tilde{c}_{23} & \partial\tilde{\sigma}_{23}/\partial\tilde{c}_{13} \\ \partial\tilde{\sigma}_{13}/\partial\tilde{c}_{11} & \partial\tilde{\sigma}_{13}/\partial\tilde{c}_{22} & \partial\tilde{\sigma}_{13}/\partial\tilde{c}_{33} & \partial\tilde{\sigma}_{13}/\partial\tilde{c}_{12} & \partial\tilde{\sigma}_{13}/\partial\tilde{c}_{23} & \partial\tilde{\sigma}_{13}/\partial\tilde{c}_{13} \end{bmatrix}. \tag{4.13}$$

This definition permits us to express the element tangent matrix as:

$$\underline{k}^e = \int_{\mathcal{S}_e} 2\ \underline{\boldsymbol{B}}^T\ \underline{\hat{\boldsymbol{D}}}\ \underline{\boldsymbol{B}}\ \underline{\boldsymbol{f}}^T - \left(\int_{\mathcal{S}_e} \underline{\boldsymbol{b}}^T \right) \frac{\kappa}{v_e} \left(\int_{\mathcal{B}_e} J^2\ \underline{\boldsymbol{b}}\ \underline{\boldsymbol{F}} \right), \tag{4.14}$$

where

$$\underline{\hat{\boldsymbol{D}}} = j^{-2/3} \left(\underline{\tilde{\boldsymbol{D}}} - \frac{1}{3}\ \underline{\tilde{\boldsymbol{D}}}\ \underline{\boldsymbol{c}}\ \underline{\boldsymbol{c}}^{-T} \right) \tag{4.15}$$

and $\mathcal{S}_e$ and $\mathcal{B}_e$ represent the spatial and reference element domain.

Remark 4.4.

To convert a standard forward element to an inverse element one merely needs to replace the tangent matrix by (4.14) and evaluate the internal force vector using the stresses in terms of the inverse motion. □

§5. Illustrations: Incompressible Neo-Hookean Material

In this section we provide illustrative examples of the inverse approach. All problems are 2D plane strain using a constant pressure four node quadrilateral and a Neo-Hookean constitutive relationship with the following strain energy function

$$W = \frac{\mu}{2}(\mathrm{tr}\,[\tilde{\boldsymbol{C}}] - 3)\,, \tag{5.1}$$

and the penalized constraint $1/j - 1 = 0$. In the above, $\tilde{\boldsymbol{C}} = \tilde{\boldsymbol{F}}^T\tilde{\boldsymbol{F}}$ and μ is a constitutive parameter. Given (5.1), the stress contribution

$$\tilde{\boldsymbol{\sigma}} = \mu\tilde{\boldsymbol{c}}^{-1} \tag{5.2}$$

and the tangent operator

$$\frac{\partial\tilde{\boldsymbol{\sigma}}}{\partial\tilde{\boldsymbol{c}}} = -\mu\mathbb{I}_{\tilde{c}^{-1}}\,, \tag{5.3}$$

where in index notation

$$\mathbb{I}_{\tilde{c}^{-1}} \rightarrow \mathbb{I}^{ijkl}_{\tilde{c}^{-1}} = \tfrac{1}{2}(\tilde{c}^{-1}_{ik}\tilde{c}^{-1}_{jl} + \tilde{c}^{-1}_{il}\tilde{c}^{-1}_{jk}). \tag{5.4}$$

Four example problems will be shown; Cook's problem, thin walled cylinder inflation, design of a rubber form, and design of a seal pressed into a wedge channel. The first two problems illustrate the elements ability to exhibit behaviors which are commonly dominated by the "locking" phenomena. Success of the method is shown for the cylinder inflation problem by comparison to (approximate) analytic results and in Cook's problem by comparison of the undeformed shape resulting from the inverse problem with a forward motion calculation. The last two problems illustrate practical uses for the method.

5.1. Cook's Problem. In this example we utilize a solution from a forward calculation as the initial conditions for an inverse problem and attempt to recover the initial conditions of the forward problem. In the forward problem, we consider a tapered panel clamped on the left edge and subjected to a shear traction on the opposite end. This problem is similar to "Cook's membrane problem" (see e.g. SIMO & ARMERO [1992]) – the difference here being a follower load. This problem illustrates an elements ability to sustain bending

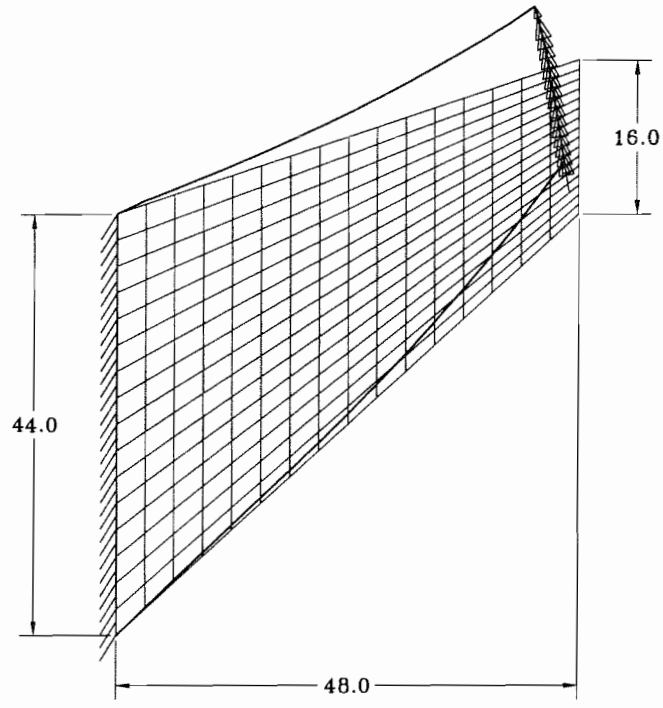

FIGURE 5.1. Cook's problem with deformed mesh outline and the calculated undeformed mesh.

and incompressible behavior. The material parameters are $\mu = 80.1938$ and penalty $\kappa = 1.0 \times 10^8$. The initial deformed configuration for the inverse problem is first found using the forward incompressible formulation described by equations (3.4)–(3.8). The deformed mesh is given by the heavy outline in Fig. **5.1**, where a follower shear traction of 4.375 was used. To test the inverse formulation we attempt to compute the shape of the reference mesh used in the forward calculation using a single time step. The solution required 6 Newton-Raphson iterations to reduce the residual by 9 orders of magnitude. The computed inverse motion gives the undeformed mesh (with interior shown) in Fig. **5.1**. The computed inverse tip displacement was found to be accurate to 0.131% and the original straight-sided panel has been clearly recovered. Better accuracy than that obtained is difficult to achieve due to the form of the chosen penalty function. Note that in the forward problem, for a quadratic volumetric energy (as has been assumed), the three-field and two-field formulations are equivalent; however, in the inverse problem with a quadratic volumetric energy, the three-field and two-field formulations are *not* equivalent. Thus, it is only reasonable to expect the inverse calculation to be accurate to the level of the difference between the two- and

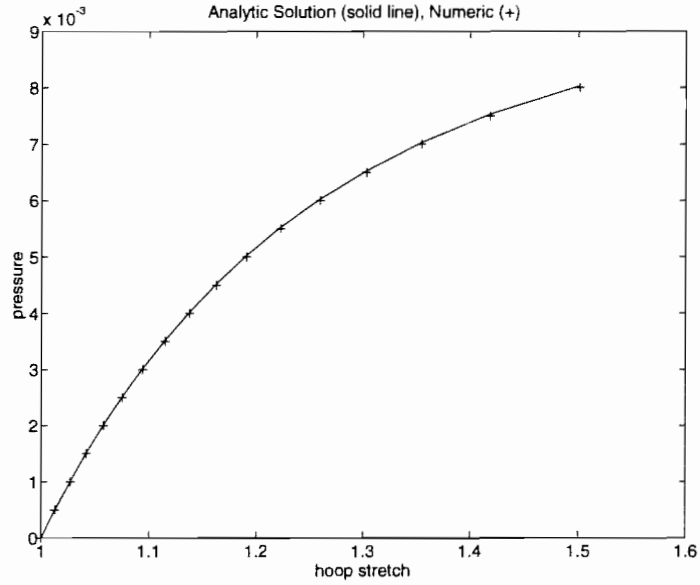

FIGURE 5.2. Forward problem for the inflation of a cylinder.

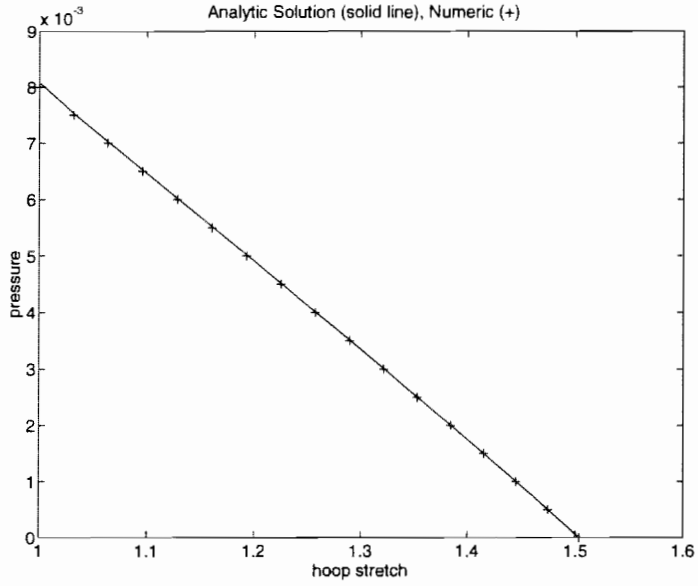

FIGURE 5.3. Inverse problem for the inflation of a cylinder, where the abscissa values are given with respect to the a priori known undeformed configuration from the analytical calculation.

three-field inverse formulations.

5.2. Inflation of a Thin Walled Infinite Cylinder. This problem has an (approximate)

analytic solution for incompressible behavior which can be used to check the method. The material parameter $\mu = 2.0000$ and penalty parameter $\kappa = 1.0 \times 10^8$.

The deformed cylinder is constructed with an inner radius of 30.024 and thickness of 0.0664. The inverse 10x10 mesh is considered for a one degree segment of the cylinder. Roller boundary conditions are defined along the lines of constant $\theta = 0^o$ and $\theta = 1^o$. A Cauchy pressure of 0.008 is applied to the inside of the cylinder. These conditions correspond to an undeformed cylinder with inner radius 20.0 and thickness 0.1 and a hoop stretch of 1.5012 according the analytical solution. For illustration and comparison we first review the forward problem. We will use a standard forward incompressible element as in the previous example, but will compare it with the analytical solution. The pressure is applied as a follower load in 16 increments of 0.0005. A plot of pressure versus stretch (Fig. **5.2**) shows the numerical solution is very close to the analytic solution thus validating the "thin-wall" assumption.

We now consider the inverse problem. In an identical manner to the forward problem we load the segment in 16 pressure increments of 0.0005. The resulting path in Fig. **5.3** is again very close to the analytical results only deviating slightly for larger values of the hoop stretch. Each solution step required 5 Newton-Raphson iterations to reduce the residual by 6 orders of magnitude. All quantities were found to be accurate to 3 significant digits with respect to the analytic solution. Note that this includes inaccuracies of the thin walled assumption in the incompressible analytic solution. We emphasize that one should not confuse the path computed with the inverse formulation with that of an unload path.

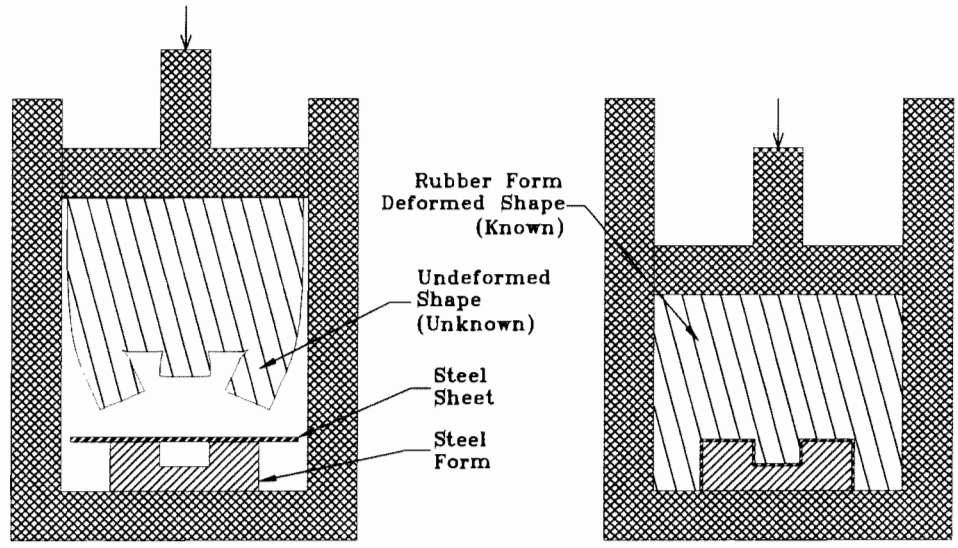

FIGURE 5.4. Design of a rubber form to be used in pressing a thin sheet of steel around a steel form. Left: unloaded press, rubber shape yet to be determined. Right: deformed shape geometry used as input to the problem.

5.3. Design of a Rubber Form. In this problem we consider the design of a rubber form to be used in pressing a thin sheet of steel around a steel form; see for example E.F. GOBEL [1974 p.181-184]. A hydraulic press is shown in Fig. **5.4** where the press is unloaded on the left and the unknown shape of the rubber form is to be determined. The given design constraint is that when a force is applied to the press, the rubber form should take up the configuration shown on the right of Fig. **5.4**. To promote an even thickness of the steel sheet after forming, we desire a uniform Cauchy pressure between the rubber form and the steel sheet.

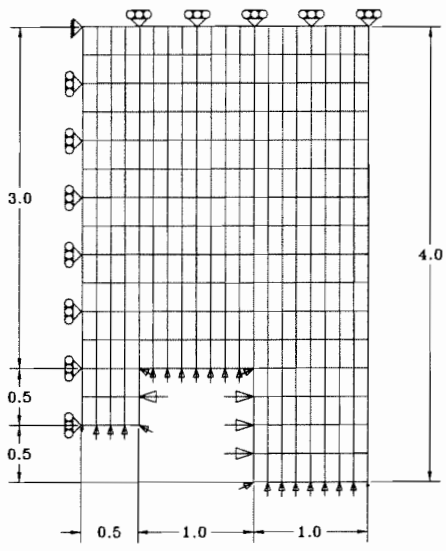

FIGURE 5.5. Finite element model (using symmetry) of deformed rubber form with desired Cauchy tractions and boundary conditions.

The finite element model uses the symmetry of the problem with the boundary conditions as shown in Fig. **5.5**. It is assumed there is no friction along the vertical walls of the press. The top portion of the rubber form is assumed to stay in contact with the hydraulic press at all times but may deform horizontally. The uniform Cauchy pressure distribution equals 100. The loading on the hydraulic press can be found from equilibrium. The material parameter $\mu = 2.0000$ and the incompressible penalty parameter $\kappa = 1.0 \times 10^5$.

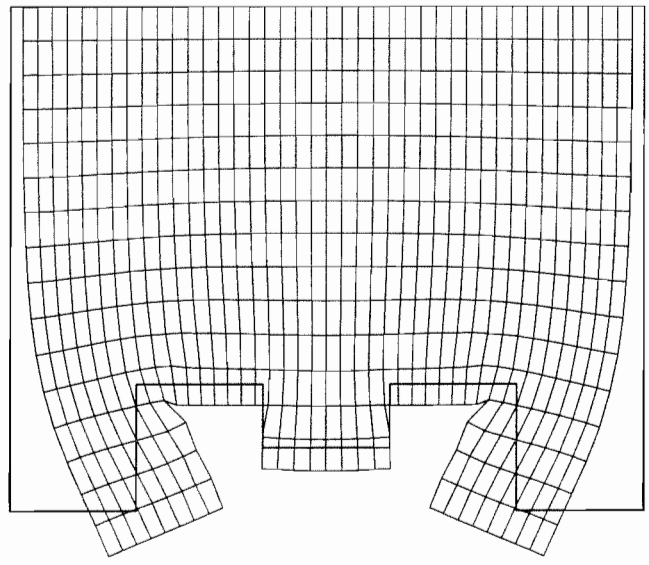

FIGURE 5.6. Rubber form with deformed mesh outlined and the calculated undeformed mesh.

The original deformed mesh is given by the heavy outline in Fig. **5.6**. The inverse solution required 6 Newton-Raphson iterations to reduce the residual by 11 orders of magnitude. The resulting undeformed mesh is shown (with interior) in Fig. **5.6**. Immediately we may conclude that the undeformed mesh leads to problems in placement and contact. Consider the left panel of Fig. **5.4**, the undeformed mesh when pressed against the sheet will not easily fit into the slots of the center or edges of the steel form. This illustrates the application of the inverse method to identify situations which lead to undesired configurations. A designer may readily conclude that the design constraints need modification.

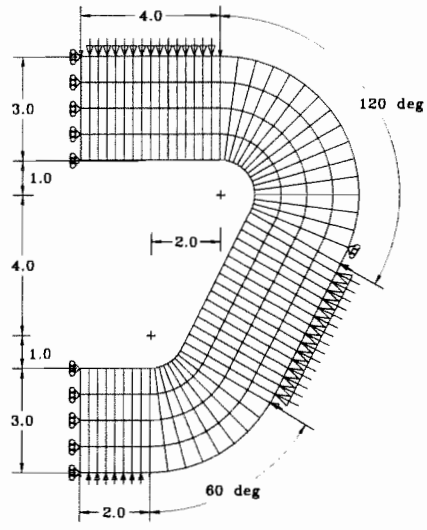

FIGURE 5.7. Finite element model (using symmetry) of a seal deformed into a wedge channel.

5.4. Seal pressed into a wedge channel. In this problem we consider the design of a rubber seal which is pressed into a wedge channel and exerts a desired pressure onto the channel; see e.g. R.H. FINNEY [1992, p.274-276]. The given deformed configuration is shown in Fig. **5.7**. The finite element model uses the symmetry of the problem with the appropriate boundary conditions as shown. It is assumed there is no friction along the walls of the seal. Additionally, we have the design constraints that there be a uniform Cauchy pressure distribution of 50 along the base, 100 along the sloped sides, and 75 along the top of the seal. The material parameter $\mu = 2.0000$ and the incompressible penalty parameter $\kappa = 1.0 \times 10^8$. Given these conditions, we wish to compute the unloaded shape of the seal.

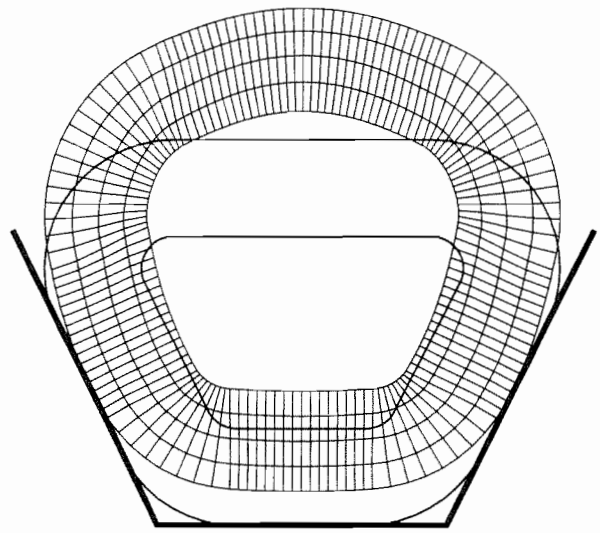

FIGURE 5.8. Seal deformed into wedge channel with deformed mesh outline and the calculated undeformed mesh.

The initial deformed mesh is given by the heavy outline in Fig. **5.8**. The inverse solution required 6 Newton-Raphson iterations to reduce the residual by 10 orders of magnitude. The resulting undeformed mesh is shown (with interior) in Fig. **5.8** shifted upward to illustrate the actual rigid body motion that will occur during insertion.

§6. Closure

This paper has presented a two-field displacement-pressure formulation for the calculation of quasi-incompressible inverse motion problems. The formulation draws on past research of SUSSMAN & BATHE [1987] and SIMO & TAYLOR [1991] and extends it to a class of inverse motion design problems. In particular, elements designed for computing forward motion problems in quasi-incompressible hyper-elasticity can be easily converted to inverse motion elements with small changes to the tangent matricies. Up to now inverse problems in quasi-incompressible elastomeric design have been considered solvable only through "trial and error correction" methods of optimization theory. By applying this formulation to active problems we have shown how to directly solve practical inverse design problems.

§ **Acknowledgments**

The authors would like to acknowledge Prof. R.L. Taylor of the University of California at Berkeley for providing access to the finite element code FEAP for the calculations presented.

§ **References**

ALLEN, P.W., LINDLEY, P.B., & PAYNE, A.R. *Use of Rubber in Engineering.* Maclaren and Sons Ltd, London, (1967).

BUI, H.D. *Inverse Problems in the Mechanics of Materials: An Introduction.* CRC Press, Boca Raton, Florida, (1994).

CHADWICK, P. "Applications of an Energy-Momentum Tensor in Elastostatics," *J. Elasticity* **5**, 249-258 (1975).

ESHELBY, J.D. "The Continuum Theory of Lattice Defects," in *Solid State Physics, Advances in Research and Applications, Vol III,* Eds: F. Seitz and D. Turnbull, Academic Press, New York, 79-144 (1956).

ESHELBY, J.D. "The Elastic Energy-Momentum Tensor," *J. Elasticity* **5**, 321-335 (1975).

FINNEY, R.H. "Finite Element Analysis," in *Engineering with Rubber, How to Design Rubber Components.* Ed: Gent, A.N., Oxford University Press, New York, (1992).

FLORY, P.J. "Thermodynamic relations for high elastic materials," *Trans. Faraday Soc.* **57**, 829-838 (1961).

GOBEL, E.F. & BRICHTA, A.M. *Rubber Spring Design.* Newnes-Butterworths, Kingsway, London, (1974).

GOVINDJEE, S. & MIHALIC, P.A. "Computational Methods for Inverse Problems in Finite Elastostatics," *Comp. Meth. Appl. Mech. Engng.* **136**, 47-57 (1996).

LUENBERGER, D.G. *Linear and Nonlinear Programming.* Addison Wesley, Menlo Park, CA, (1984).

OGDEN, R.W. *Non-linear Elastic Deformations.* Ellis Horwood Limited, Chichester, England, (1984).

SHIELD, R.T. "Inverse Deformation Results in Finite Elasticity," *Z. Agnew. Math. Phys.* **18**, 381-389 (1967).

SIMO, J.C. & TAYLOR, R.L. "Quasi-incompressible Finite Elasticity in Principal Stretches: Continuum Basis and Numerical Algorithms," *Comp. Meth. Appl. Mech. Engng.* **85**, 273-310 (1991).

SIMO, J.C. & ARMERO, F. "Geometrically nonlinear enhanced strain mixed methods and the method of incompatible modes," *Int. J. Numer. Meth, Engng.* **33**, 1413-1449 (1992).

SUSSMAN, T. & BATHE, K.J. "A finite element formulation for nonlinear incompressible elastic and inelastic analysis, " *Comput. & Structures* **26**, 357-109 (1987).

TRELOAR, L.R.G. *The Physics of Rubber Elasticity, 3rd Edition.* Oxford Univ. Press, Oxford, UK, (1975).

YAMADA, T. "Finite Element Procedure of Initial Shape Determination for Rubber-like Materials," *Res. Lab. Eng. Mat. Tokyo Inst. Tech.* Report No. 20, (1995).

§Appendix A: Three Field Formulation

For completeness we include the inverse form of the three field formulation of SIMO & TAYLOR [1991]. This formulation may also be combined with an Augmented Lagrangian approach to enforce the constraint to a high degree without numerical ill-conditioning. In the forward problem, the Jacobian of the deformation gradient is included as an additional independent field. In the inverse problem we will use the Jacobian of the inverse motion as a third field. Thus, the strong form equations for the three field inverse (penalized) incompressible problem are given by: for all $x \in \mathcal{S}$

$$j = \theta, \tag{A.1}$$

$$p = \kappa(1/\theta - 1), \tag{A.2}$$

and

$$\text{div}[\tilde{\boldsymbol{\sigma}} + p\mathbf{1}] + \widehat{\boldsymbol{b}} = 0 \quad \text{and} \quad \boldsymbol{\sigma} = \boldsymbol{\sigma}^T; \tag{A.3}$$

for all $\boldsymbol{x} \in \partial\mathcal{S}_t$

$$\boldsymbol{\sigma}\boldsymbol{n} = \bar{\boldsymbol{t}}\,; \tag{A.4}$$

for all $\boldsymbol{x} \in \partial\mathcal{S}_\varphi$

$$\boldsymbol{\varphi} = \bar{\boldsymbol{\varphi}}.\,, \tag{A.5}$$

The constitutive relation is given by:

$$\tilde{\boldsymbol{\sigma}} = \boldsymbol{P}(\tilde{\boldsymbol{f}}^{-1})\tilde{\boldsymbol{f}}^{-T}. \tag{A.6}$$

The weak form equations for the inverse incompressible problem are derived by multiplying (A.1) - (A.3) by arbitrary admissible weighting functions, integrating over the domain, and performing integration by parts on the result. The resulting weak form expressions are,

$$\tilde{G}_p(\boldsymbol{\varphi}, \theta; \beta) = \int_{\mathcal{S}} [j - \theta]\beta = 0 \tag{A.7}$$

$$\tilde{G}_\theta(\theta, p; \alpha) = \int_{\mathcal{S}} [\kappa(1/\theta - 1) - p]\,\alpha = 0, \tag{A.8}$$

and

$$\tilde{G}_\varphi(\boldsymbol{\varphi}, p; \boldsymbol{\eta}) = \int_{\mathcal{S}} [\tilde{\boldsymbol{\sigma}} : grad(\boldsymbol{\eta}) + p\ \text{div}(\boldsymbol{\eta})] + G_{ext} = 0 \tag{A.9}$$

where $\boldsymbol{\eta} : \mathcal{S} \longrightarrow \mathbb{R}^3$ and $\boldsymbol{\eta} = 0$ on $\partial\mathcal{S}_\varphi$, $\beta : \mathcal{S} \longrightarrow \mathbb{R}$, $\alpha : \mathcal{S} \longrightarrow \mathbb{R}$, and G_{ext} contains the contribution of the tractions $\bar{\boldsymbol{t}}$ and body forces $\widehat{\boldsymbol{b}}$.

The finite element formulation of the weak form problem defined by (A.7) - (A.9) can be solved using suitable approximations for β, α, $\boldsymbol{\eta}$, θ, p and $\boldsymbol{\varphi}$. By assuming a constant approximation per element for β, α, θ, and p we can solve (A.7) explicitly for θ_e as

$$\theta_e(\boldsymbol{\varphi}) = \frac{1}{v_e}\int_{\mathcal{S}_e} j \tag{A.10}$$

and also solve (A.8) explicitly for p_e as

$$p_e(\boldsymbol{\varphi}) = \frac{1}{v_e}\int_{\mathcal{S}_e} \kappa(\frac{1}{\theta_e} - 1), \tag{A.11}$$

where $\mathcal{S}_e$ refers to an individual element domain and v_e is the "spatial element volume." We can then substitute (A.11) back into (A.9) to arrive at a single weak form expression,

$$G(\boldsymbol{\varphi};\boldsymbol{\eta}) = \tilde{G}_{\varphi}(\boldsymbol{\varphi}, p_e(\boldsymbol{\varphi});\boldsymbol{\eta}) = 0. \tag{A.12}$$

Equation (A.12) represents a set of non-linear equations which can be solved for the motion $\boldsymbol{\varphi}$.

The Newton-Raphson method can be applied to (A.12) to solve for the unknown motion. The needed tangent operator for using this technique in terms of an admissible variation $\boldsymbol{\nu} : \mathcal{B} \longrightarrow \mathbb{R}^3$ ($\boldsymbol{\nu} = 0$ on $\partial\mathcal{S}_{\varphi}$) is given by

$$\begin{aligned} D_1 G(\boldsymbol{\varphi}^{(k)};\boldsymbol{\eta})[\boldsymbol{\nu}] = &\int_{\mathcal{S}_e} 2\,\mathrm{sym}[\mathrm{grad}(\boldsymbol{\eta})] : \mathrm{DEV}\left[\frac{\partial\tilde{\boldsymbol{\sigma}}}{\partial\tilde{\mathbf{c}}}\right] : \mathrm{sym}[\boldsymbol{f}^T\mathrm{grad}(\boldsymbol{\nu})] \\ &- \left(\int_{\mathcal{S}_e} \mathrm{div}(\boldsymbol{\eta})\right)\frac{\kappa}{\theta^2 v_e}\left(\int_{\mathcal{B}_e} \mathrm{DIV}(\boldsymbol{\nu})\right). \end{aligned} \tag{A.13}$$